

Adaptive Near-Optimal Compensation in Lossy Polyphase Power Systems

Ronald D. Hernández, Hanoch Lev-Ari, Aleksandar M. Stanković and Edwin A. Marengo
Northeastern University

Department of Electrical and Computer Engineering, Boston, MA 02115, USA

Email: {llevari, rhernand, astankov, emarengo}@ece.neu.edu

Abstract—The paper provides a formulation and solution for the problem of optimizing power flows in polyphase power systems with significant source (line) impedance. An optimal solution considering significant line impedance has been already obtained in recent works. Unfortunately, it relies on network and load parameters that are not easy to determine during operation. This motivates our approach in searching for a sub-optimal easy-to-implement solution that relies only on measurements of the load voltage and current.

I. INTRODUCTION

The role of compensation in power system efficiency optimization is to reduce the power consumption of the (Thevenin equivalent) source (or “line”) impedance, so that most of the source power is delivered to the load (Fig. 1). A classical result by Fryze [1] states that when the voltage drop across the line impedance is negligible in comparison with the load voltage, i.e., when $\|v_s(t) - v(t)\| \ll \|v(t)\|$ then the smallest (in rms) possible source current $i_s(t)$ is

$$i_F(t) = \frac{P_{load}^{(u)}}{\|v\|^2} v(t) \quad (1)$$

where $P_{load}^{(u)}$ is the original real (average) power delivered to the load without compensation (uncompensated load), and $\|v\|$ denotes the rms value of a waveform $v(t)$. Recently we have put compensation (with negligible voltage drop) in a convenient geometric (Hilbert space) setting, and determined optimal solutions under unequal line resistances and bandwidth limitation on the compensator current [2–4].

However, when the source impedance becomes significant the traditional Fryze current is no longer the smallest line current that supplies the same real power to the load as the original load current. In that case, every adjustment in the compensator current results in a change of voltage load, which in turn, requires further adjustments in compensator current. Furthermore, the theoretically-optimal compensator, as derived in [5], [6], depends on both the equivalent source impedance and the current-voltage characteristic of the load. Such information is usually difficult to obtain, especially in view of the time-varying nature of network parameters.

In this paper we introduce an adaptive near-optimal compensation scheme that relies only on measurements of the load voltage and current. Our compensator tracks variations in both network and load conditions, continuously adjusting the polyphase waveform $i_{comp}(t)$ so as to reduce the power dissipated in the source impedance, for both linear and nonlinear loads. To be specific, this compensation algorithm allows precise control of P_{comp} , the real power flowing out of the compensator, as well as P_{load} , the real power delivered to the compensated load (i.e., $P_{load} = P_{load} - P_{comp}$), while reducing P_{line} , the power dissipated in the source impedance, to within a few percent of its theoretical minimum.

The heart of our adaptive compensation scheme is the concept of *quadrature Fryze* compensation (*quad-Fryze* for short), which was introduced in [5]. The objective of a quad-Fryze compensator is to

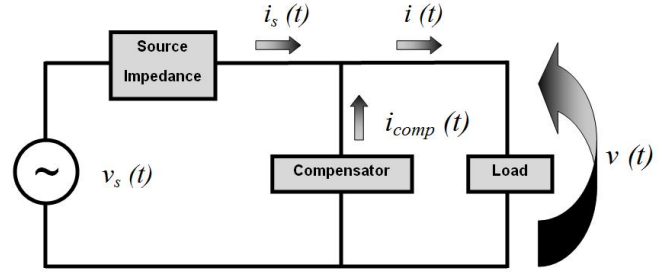


Fig. 1. Load compensation in a power delivery system.

adjust $i_{comp}(t)$ so that the compensated load is linear and time-invariant with a current-voltage characteristic given by

$$i_s(t) = \alpha v(t) - \beta \mathcal{H}\{v(t)\}. \quad (2)$$

Here α, β are real-valued coefficients and $\mathcal{H}\{\cdot\}$ represents the Hilbert transform of a signal. In other words, the compensated line current is a linear combination of the load voltage $v(t)$ and its Hilbert transform $\mathcal{H}\{v(t)\}$. We call this compensation method “quadrature Fryze” because the Hilbert transform imparts a 90° phase delay to $v(t)$. It was demonstrated in [5] that the performance of this (implicit) compensation scheme is often very close to the theoretical optimum in the presence of significant source impedance.

The two parameters α and β in (2) can be used to control the values of P_{comp} and P_{load} . Our adaptive compensation algorithm adjusts these two control parameters to achieve the prescribed P_{comp}, P_{load} values, relying in the process only on information about the load current and voltage.

II. PROBLEM FORMULATION

The Hilbert space terminology of [2] is used here to formulate our objectives and derive our results. Thus $v(t)$ and $i(t)$ are row vectors representing polyphase load voltage and current, respectively, which we view as elements in a Hilbert space of n -phase, T -periodic, square-integrable waveforms, with the inner product represented by

$$\langle x, y \rangle \stackrel{\text{def}}{=} \frac{1}{T} \int_T x(t) y(t)^\top dt \quad (3)$$

where the superscript \top denotes transposition.

This inner product can also be evaluated in terms of the Fourier coefficients X_l, Y_l of the polyphase waveforms $x(t), y(t)$, namely

$$\langle x, y \rangle = \Re\{\mathcal{X}\mathcal{Y}^H\} \quad (4)$$

where the subscript H indicates conjugate transpose, and \mathcal{X} is a one-sided phasor array, viz.,

$$\mathcal{X} \stackrel{\text{def}}{=} [X_0 \quad \sqrt{2}X_1 \quad \sqrt{2}X_2 \quad \dots] \quad (5)$$

consisting of the row-vector Fourier coefficients

$$X_l = \frac{1}{T} \int_T x(t) e^{-j\omega t} dt \quad (6)$$

and similarly for the phasor array \mathcal{Y} , which represents the waveform $y(t)$.

The behavior of the power delivery system of Fig. 1 is determined by the current-voltage characteristic of the load and the (frequency-domain) circuit equations

$$\mathcal{I} = \mathcal{I}_s + \mathcal{I}_{comp} \quad (7a)$$

$$\mathcal{V} = \mathcal{V}_s - \mathcal{I}_s \mathcal{Z}_s \quad (7b)$$

where \mathcal{Z}_s is a complex-valued matrix representing the linear time-invariant source impedance, and \mathcal{I} , \mathcal{I}_s , \mathcal{I}_{comp} , \mathcal{V} , \mathcal{V}_s are the phasor arrays associated with the polyphase waveforms $i(t)$, $i_s(t)$, $i_{comp}(t)$, $v(t)$, $v_s(t)$, respectively.

These circuit equations establish a one-to-one correspondence between the source current \mathcal{I}_s and the compensator current \mathcal{I}_{comp} (when we consider a fixed \mathcal{V}_s , \mathcal{Z}_s and \mathcal{Y}). This is straightforward to establish for a linear load, where $\mathcal{I} = \mathcal{V}\mathcal{Y}$ with the matrix \mathcal{Y} representing the load admittance. Indeed, from (7) we can get

$$\mathcal{I}_s = (\mathcal{V}_s - \mathcal{I}_s \mathcal{Z}_s) \mathcal{Y} - \mathcal{I}_{comp} \quad (8a)$$

so that

$$\mathcal{I}_s = (\mathcal{V}_s \mathcal{Y} - \mathcal{I}_{comp}) (I + \mathcal{Z}_s \mathcal{Y})^{-1}. \quad (8b)$$

In the linear case, nonsingularity of the matrix $(I + \mathcal{Z}_s \mathcal{Y})$ is the only condition needed to ensure one-to-one correspondence between \mathcal{I}_s and \mathcal{I}_{comp} . This condition is almost always met, either because $\|\mathcal{Z}_s \mathcal{Y}\|$ is small, or because the eigenvalues of $\mathcal{Z}_s \mathcal{Y}$ have a positive real part.

The performance of any compensator, including the one we introduce in this paper, can be evaluated in terms of three real (average) power quantities:

- The power P_{line} dissipated in the equivalent source impedance, viz.,

$$P_{line} \stackrel{\text{def}}{=} \mathcal{I}_s \mathcal{R}_s \mathcal{I}_s^H \quad (9a)$$

where

$$\mathcal{R}_s \stackrel{\text{def}}{=} \frac{1}{2} \{ \mathcal{Z}_s + \mathcal{Z}_s^H \}. \quad (9b)$$

- The power P_{load} delivered to the compensated load, viz.,

$$P_{load} \stackrel{\text{def}}{=} \Re \{ \mathcal{I}_s \mathcal{V}^H \} = \Re \{ \mathcal{I}_s \mathcal{V}_s^H \} - P_{line}. \quad (10)$$

- The power P_{comp} flowing out of the compensator, viz.,

$$\begin{aligned} P_{comp} &\stackrel{\text{def}}{=} \Re \{ \mathcal{I}_{comp} \mathcal{V}^H \} \\ &= \Re \{ \mathcal{I} \mathcal{V}^H \} - P_{load}. \end{aligned} \quad (11)$$

Notice that our expressions use \mathcal{I}_s , rather than \mathcal{I}_{comp} , as the independent variable.

III. OPTIMAL PERFORMANCE CURVES

In order to evaluate the performance of our adaptive compensation scheme in the presence of non-negligible source impedance, we shall use the concept of optimal performance curves, originally introduced in [6]. The first step towards the construction of such curves is to obtain explicit expressions for the three criteria of interest — P_{line} , P_{load} and P_{comp} — as a function of the source current \mathcal{I}_s .

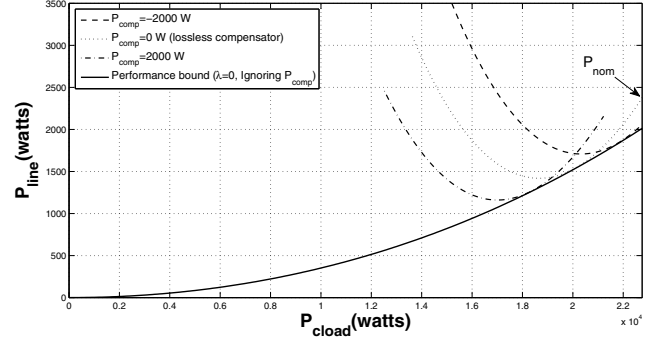


Fig. 2. Optimal performance benchmarks ($P_{nom} = 22,750W$).

Following the practice in [6] we use here the normalized independent vector variable

$$\mathcal{X} \stackrel{\text{def}}{=} \frac{1}{\sqrt{P_{nom}}} \mathcal{I}_s \mathcal{R}_s^{1/2} \quad (12)$$

where P_{nom} is the nominal power that would be delivered to the load in the absence of the line impedance. This allows us to obtain the expressions

$$\frac{P_{line}}{P_{nom}} = \mathcal{X} \mathcal{X}^H = \|\mathcal{X}\|^2 \quad (13)$$

and

$$\frac{P_{load}}{P_{nom}} = \mathcal{X} \xi^H + \xi \mathcal{X}^H - \mathcal{X} \mathcal{X}^H \quad (14a)$$

where

$$\xi \stackrel{\text{def}}{=} \frac{1}{2\sqrt{P_{nom}}} \mathcal{V}_s \mathcal{R}_s^{-H/2}. \quad (14b)$$

Notice that

$$\begin{aligned} \frac{P_{load}}{P_{nom}} &= 2\Re \{ \mathcal{X} \xi^H \} - \frac{P_{line}}{P_{nom}} \\ &\leq 2\|\mathcal{X}\| \|\xi\| - \frac{P_{line}}{P_{nom}} \end{aligned} \quad (15)$$

which gives us the universal performance bound of [6], viz.,

$$\frac{P_{load}}{P_{nom}} \leq \sqrt{\frac{P_{sc}}{P_{nom}}} \cdot \sqrt{\frac{P_{line}}{P_{nom}}} - \frac{P_{line}}{P_{nom}} \quad (16)$$

where $P_{sc} \stackrel{\text{def}}{=} \mathcal{V}_s \mathcal{R}_s^{-1} \mathcal{V}_s^H$. The universal performance bound (solid line in Fig. 2) describes the theoretical minimum for P_{line} as a function of P_{load} , with no constraints on P_{comp} .

Thus feasible (P_{line}, P_{load}) combinations, under any compensation scheme, must satisfy the inequality (16), and correspond to points above the universal performance curve. Notice that this curve depends only on the source voltage and impedance, and is completely independent of the load.

In contrast, the expression for P_{comp} is explicitly dependent on the load, as is the value of P_{nom} . The case of a linear load was analyzed in [6], where it was shown that

$$P_{nom} \stackrel{\text{def}}{=} \mathcal{V}_s \mathcal{G} \mathcal{V}_s^H \quad (17a)$$

where

$$\mathcal{G} \stackrel{\text{def}}{=} \frac{1}{2} (\mathcal{Y} + \mathcal{Y}^H), \quad (17b)$$

as well as

$$\frac{P_{comp}}{P_{nom}} = \mathcal{X} A \mathcal{X}^H - \mathcal{X} \eta^H - \eta \mathcal{X}^H + 1 \quad (18a)$$

where

$$A \stackrel{\text{def}}{=} I + (\mathcal{R}_s^{-1/2} \mathcal{Z}_s) \mathcal{G} (\mathcal{R}_s^{-1/2} \mathcal{Z}_s)^H \quad (18b)$$

and

$$\eta \stackrel{\text{def}}{=} \frac{1}{\sqrt{P_{nom}}} \mathcal{V}_s \left[\frac{1}{2} I + \mathcal{G} \mathcal{Z}_s^H \right] \mathcal{R}_s^{-H/2}. \quad (18c)$$

For a nonlinear load we can determine P_{comp} only by numerical calculation, which solves the nonlinear equations that determine the map $\mathcal{I}_s \rightarrow \mathcal{V} \rightarrow \mathcal{I} \rightarrow \mathcal{I}_{comp} \rightarrow P_{comp}$.

Our main objective here is to determine *cross-section curves* (dashed, dotted and das-dot lines in Fig. 2) corresponding to fixed values of P_{comp} . Here we shall limit our discussion to linear loads, for which one needs to solve a quadratic cost, quadratically-constrained optimization problem. As explained in [6], this can be accomplished via the Lagrange multiplier method, resulting in the optimal (scaled) source current

$$\mathcal{X}_{opt} = (\nu \xi + \lambda \eta) [(1 + \nu)I + \lambda A]^{-1} \quad (19)$$

where ν, λ are the Lagrange multipliers. Cross-section curve is obtained by finding all the (ν, λ) pairs that satisfy the constraint

$$\mathcal{X}_{opt} A \mathcal{X}_{opt}^H - 2\Re\{\mathcal{X}_{opt} \eta^H\} + 1 = \frac{P_{comp}}{P_{nom}} \quad (20)$$

for a given P_{comp} value.

The cross-section curves described in Fig. 2 allow us to obtain the best trade-off between P_{line} and P_{load} achievable for the compensator. Each cross-section curve describes the theoretical minimum for P_{line} as a function of P_{load} for a prescribed level of P_{comp} .

As an example, consider the case of a three-phase induction machine rated at $25kW$, supplied from an unbalanced source (variations of roughly 10% in magnitude and phase, with no zero sequence) that contains the fundamental and the fifth harmonic. The numerical values are the same as in [5].

We now observe that the smallest P_{line} achievable with a lossless compensator (dotted line in Fig. 2) is $1,418W$ and the corresponding $P_{load} = 18,660W$. If we attempt to supply the nominal power to the load, which in our example corresponds to $P_{load} = 22,750W$, then it is necessary to compromise on the power loss in the source impedance, i.e., P_{line} has to be increased to $2,376W$.

The family of all possible cross-section curves, for all possible values of P_{comp} is bounded from below by the universal performance bound given by (16). It can also be determined directly from (19) by setting $\lambda = 0$.

IV. QUAD-FRYZE COMPENSATION

Our proposed adaptive compensation scheme is based on the concept of quad-Fryze compensation. A quad-Fryze compensator is one that achieves, in steady-state,

$$i_s(t) = \alpha v(t) - \beta \mathcal{H}\{v(t)\}, \quad (21)$$

for some constants α, β . In the frequency domain this translates into

$$\mathcal{I}_s = \gamma \mathcal{V}, \quad \gamma = \alpha + j\beta. \quad (22)$$

This means that the compensated polyphase load is linear, time-invariant and balanced with no coupling between phases, and with a constant star-connected admittance equal to γ .

The steady-state phasor relation (22) implies, in conjunction with (7b), that the voltage across the load is given by

$$\mathcal{V} = \mathcal{V}_s (I + \gamma \mathcal{Z}_s)^{-1} \quad (23)$$

for the most general (e.g., nonlinear) load. Notice that \mathcal{I}_s , and consequently \mathcal{V} , rely on two real-valued design parameters — α and

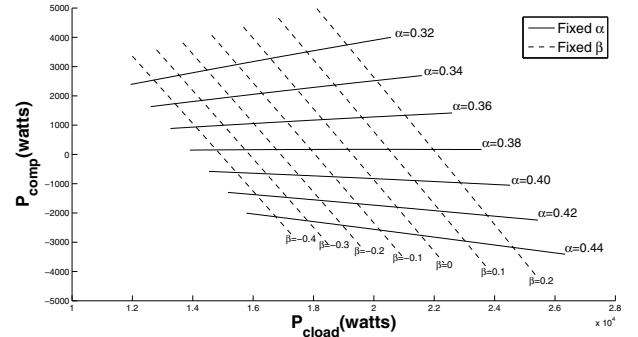


Fig. 3. Mapping of α, β into $P_{comp} - P_{load}$ plane.

β — which makes it possible to satisfy the two desired constraints on P_{comp} and P_{load} . Actually, there exists a one-to-one correspondence between the pair (α, β) and the pair (P_{comp}, P_{load}) , as illustrated in Fig. 3. In particular, the line $\alpha = 0.38$ very nearly corresponds to $P_{comp} = 0$: this suggests that our objective of lossless compensation can be achieved by controlling the value of α . Once the constraint of $P_{comp} = 0$ has been satisfied (in this example by setting $\alpha \approx 0.38$), we are free to vary the value of β so as to achieve a desired value of P_{load} . Notice that the relation between β and P_{load} , along a line of constant α , is monotone increasing.

The plotting of Fig. 3, and the choices for α and β values rely on specific information about network and load parameters, which makes a direct implementation of the quad-Fryze compensator rather impractical. However, our *adaptive algorithm* adjusts the values of α and β to achieve the prescribed P_{comp} and P_{load} values, relying in the process only on measurements of the load current and voltage (see Sec. V).

The values of P_{line} , P_{comp} and P_{load} associated with a quad-Fryze compensator can be evaluated via (23) and the expressions (9) – (11). Thus

$$P_{line} = |\gamma|^2 \mathcal{V} \mathcal{R}_s \mathcal{V}^H, \quad P_{load} = \alpha \|\mathcal{V}\|^2 \quad (24a)$$

for any load. Also, for a *linear load*,

$$P_{comp} = \mathcal{V} (\mathcal{G} - \alpha I) \mathcal{V}^H. \quad (24b)$$

The quad-Fryze compensator becomes optimal (with $\beta = 0$) when $\frac{\|\mathcal{V}_s - \mathcal{V}\|}{\|\mathcal{V}_s\|} \downarrow 0$. However, we will demonstrate via an example in Sec. V that it is very nearly optimal even in the presence of a non-negligible line impedance. Indeed, the quality of the “match” between quad-Fryze and theoretically optimal performance depends on how “non-negligible” \mathcal{Z}_s is.

The expressions (24) allow us to determine the quad-Fryze equivalent of the cross-section curves of Fig. 2, i.e., the $P_{line} - P_{load}$ tradeoff achieved by a quad-Fryze compensator with a prescribed value of P_{comp} . The results for our induction machine example indicate that the performance of the quad-Fryze compensator is almost indistinguishable from the theoretical optimum (see Fig. 4, dashed and solid curves represent quad-Fryze approaches while dotted and dash-dot curves represent optimal approaches), i.e., less than 3% of difference between quad-Fryze and optimal P_{line} values when $0.60P_{nom} \leq P_{load} \leq P_{nom}$ for all P_{comp} .

The basic challenge is to implement the quad-Fryze compensator, i.e., to find \mathcal{I}_{comp} such that $\mathcal{I}_s = \gamma \mathcal{V}$ is achieved without knowing \mathcal{Z}_s or the load characteristics. We can rely however on our ability to measure \mathcal{I}, \mathcal{V} whenever needed. In the following section we present

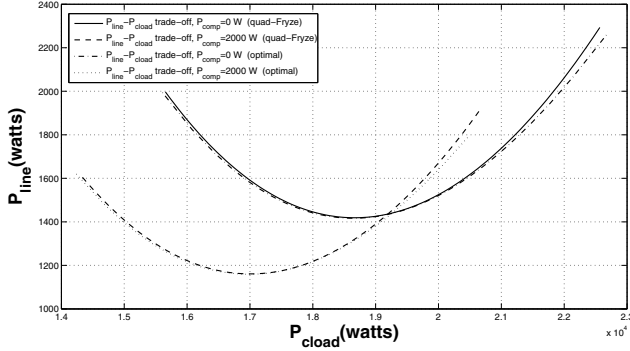


Fig. 4. Comparison between a quad-Fryze compensator solution versus an optimal solution ($P_{nom} = 22,750W$).

an adaptive version of the quad-Fryze compensator that uses only \mathcal{I} , \mathcal{V} .

V. ADAPTIVE NEAR-OPTIMAL COMPENSATOR

The approach we use is a repeated application of the optimized solution for the negligible impedance case, i.e., the ideal case in which changes in \mathcal{I}_{comp} do not change load conditions. Thus our adaptive procedure can be summarized as follows:

(i) Given the current and voltage of the load, $\{\mathcal{I}(k), \mathcal{V}(k)\}$, set the compensator to

$$\mathcal{I}_{comp}(k+1) = \mathcal{I}(k) - \gamma \mathcal{V}(k). \quad (25)$$

(ii) Wait until the network transients have died off and the load has stabilized at a new current-voltage pair, $\{\mathcal{I}(k+1), \mathcal{V}(k+1)\}$, then apply (25) again and again.

The iteration (25) generates a sequence $(\mathcal{I}(k), \mathcal{V}(k))$ of load currents and voltages, that converges (under mild technical constraints) to an equilibrium point of (25). This equilibrium is

$$\mathcal{I}_s(\infty) = \mathcal{I}(\infty) - \mathcal{I}_{comp}(\infty) = \gamma \mathcal{V}(\infty). \quad (26)$$

so that our objective of implementing quad-Fryze compensation, for a prescribed value of γ , is achieved.

A. Equilibrium and convergence

In order to understand the application of the concept of equilibrium to our approach, it is necessary to take a look at the relation

$$\mathcal{I}_{comp} = \mathcal{I} - \gamma \mathcal{V} \implies \mathcal{I}_s = \mathcal{I} - \mathcal{I}_{comp} = \gamma \mathcal{V} \quad (27)$$

so the equilibrium point is a quad-Fryze compensator. Notice that for a fixed γ this is unique, because we know from Sec. IV that the condition $\mathcal{I}_s = \gamma \mathcal{V}$ is satisfied by a single set of voltages and currents determined by $\mathcal{V} = \mathcal{V}_s(I + \gamma \mathcal{Z}_s)^{-1}$.

We turn now our discussion to the convergence analysis of our adaptive compensator. Here we shall focus on the linear load case in order to achieve our objective.

As mentioned before, setting \mathcal{I}_{comp} will result in a change of the voltage load and current which is governed by the circuit equations (7) in conjunction with $\mathcal{I} = \mathcal{V}\mathcal{Y}$ so that once the transients have died off we obtain

$$\mathcal{V} = (\mathcal{V}_s + \mathcal{I}_{comp} \mathcal{Z}_s)(I + \mathcal{Y} \mathcal{Z}_s)^{-1}, \quad (28)$$

where it is evident that the natural response of the network maps every given \mathcal{V}_s and \mathcal{I}_{comp} pair into a load voltage \mathcal{V} .

Using the linear load relation $\mathcal{I} = \mathcal{V}\mathcal{Y}$, we can deduce from (25) that the compensator current during the adaptation process is given by

$$\mathcal{I}_{comp}(k+1) = \mathcal{V}(k)[\mathcal{Y} - \gamma(k)I]. \quad (29)$$

Combining the compensator current setting (29) with the network response (28) results in a new load voltage

$$\mathcal{V}(k+1) = \mathcal{V}_s(I + \mathcal{Y} \mathcal{Z}_s)^{-1} + \mathcal{V}(k)\mathcal{A}, \quad (30a)$$

where \mathcal{A} is a shorthand notation, viz.,

$$\mathcal{A} \stackrel{\text{def}}{=} (\mathcal{Y} - \gamma I) \mathcal{Z}_s (I + \mathcal{Y} \mathcal{Z}_s)^{-1}. \quad (30b)$$

We define the load voltage error as

$$\epsilon(k) = \mathcal{V}(k) - \mathcal{V}(\infty), \quad (31)$$

so that the difference equation

$$\epsilon(k+1) = \epsilon(k)\mathcal{A} \quad (32)$$

can be obtained.

Now from (32) it is observed that $\|\epsilon(k)\| \rightarrow 0$ if, and only if, all the eigenvalues of \mathcal{A} are within the unit circle, namely, $\max\{|\lambda_i(\mathcal{A})|\} < 1$. Thus, for the case when γ is fixed, our convergence analysis reduces to the examination of the eigenvalues of the constant matrix \mathcal{A} .

Our next step is to propose an adaptive adjustment of α that will produce a prescribed value of P_{comp} (most often $P_{comp} = 0$).

B. Adaptive adjustment of α

We observe from (11) and (24a) that

$$P_{load} = \alpha \|\mathcal{V}\|^2 = \Re\{\mathcal{I}\mathcal{V}^H\} - P_{comp}. \quad (33)$$

This motivates us to use (in the adaptive algorithm)

$$\alpha(k) = \Re\{\gamma(k)\} = \frac{\Re\{\mathcal{I}(k)\mathcal{V}^H(k)\} - P_{comp,desired}}{\|\mathcal{V}(k)\|^2} \quad (34)$$

with the objective of enforcing a prescribed value on P_{comp} (which constitutes a priority over enforcing P_{load} in this step).

This means that our adaptive algorithm is, in fact,

$$\mathcal{I}_{comp}(k+1) = \mathcal{I}(k) - (\alpha(k) + j\beta)\mathcal{V}(k), \quad (35)$$

with $\alpha(k)$ given by (34)

If the convergence with this $\alpha(k)$ occurs (for a determined value of β), then the equilibrium point satisfies $\mathcal{I}_s = \gamma \mathcal{V}$ and, consequently, in steady state $P_{comp}(\infty)$ is equal to the prescribed value because then $\gamma(k) = \gamma(\infty)$, $\Re\{\mathcal{I}(k)\mathcal{V}^H(k)\} = \Re\{\mathcal{I}(\infty)\mathcal{V}^H(\infty)\}$, and so, from (34), $P_{comp}(\infty) = P_{comp,desired}$.

C. Adjustment of β

When our adaptive algorithm (34) and (35) converges, $P_{comp}(\infty) = P_{comp,desired}$, as we have demonstrated in the previous section. On the other hand, $P_{load}(\infty)$ cannot be set within this recursion, and it clearly depends on the value of β (recall Fig. 3).

When the line and load parameters \mathcal{Z}_s , \mathcal{Y} are known, we can determine the explicit relation between P_{load} and β (Fig. 5). Because this relation is smooth and monotone increasing, one can use a variety of search procedures to determine the correct β for a desired P_{load} value. Such procedures must, of course, rely only on measurable quantities such as \mathcal{I} , \mathcal{I}_s and \mathcal{V} .

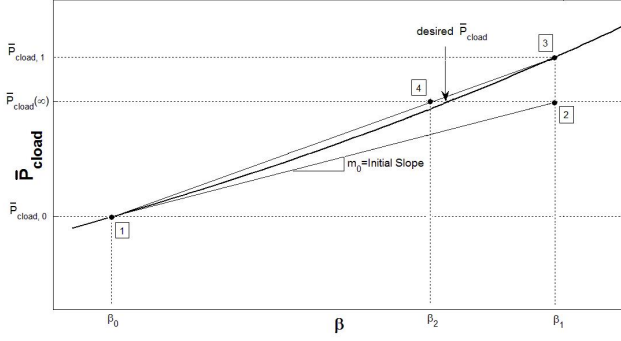


Fig. 5. Iterative adjustment of β to get desired \bar{P}_{cload} .

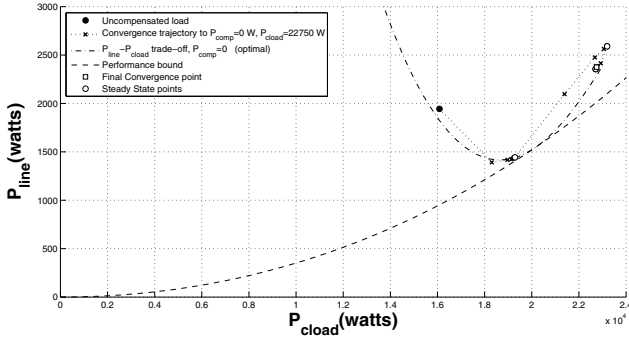


Fig. 6. Convergence trajectory of the adaptive near-optimal compensator for $P_{comp}(\infty) = 0$, $P_{cload}(\infty) = 22,750W$.

We determine β_k via the expression

$$\beta_{i+1} = \beta_i - \frac{\beta_i - \beta_{i-1}}{P_{cload,i} - P_{cload,i-1}} [\bar{P}_{cload,i} - \bar{P}_{cload,desired}], \quad (36)$$

where for computational convenience, we have replaced all P_{cload} values by their normalized equivalents, viz.,

$$\bar{P}_{cload} = \frac{P_{cload}}{P_{nom}}. \quad (37)$$

The expression given in (36) is well-known method, known as the ‘‘secant method’’ (see Fig. 5).

The recursion (36) is initialized with a choice of β_0 and β_1 . A reasonable choice for β_0 would be $\beta_0 = 0$, since it tends to generate a near-optimal value for the line loss P_{line} (see Fig. 6). The selection of β_1 has to be consistent with the monotone increasing relation mentioned before, so that $\beta_1 > \beta_0$ when $P_{cload,desired} > P_{cload,0}$, which is usually the case. One possible choice is to use a predetermined slope m_0 for the segment (β_0, β_1) — we use $m_0 = 0.56$ — so that

$$\beta_1 = \beta_0 + \frac{\bar{P}_{cload,desired} - \bar{P}_{cload,0}}{m_0}. \quad (38)$$

Now our procedure is completely specified: for each β_i we run the adaptive algorithm (35) until convergence is achieved. The corresponding steady state P_{cload} value, viz., $P_{cload,i}(\infty) = \Re \{ \mathcal{I}_s(\infty) \mathcal{V}^H(\infty) \}$ is then used to determine β_{i+1} via (36) for $i \geq 2$, or to determine β_1 via (38).

Plots in Fig. 6 provide an example for the performance of our adaptive near-optimal compensation method. Here the dotted line simply connects the points obtained by the iterative algorithm. Notice

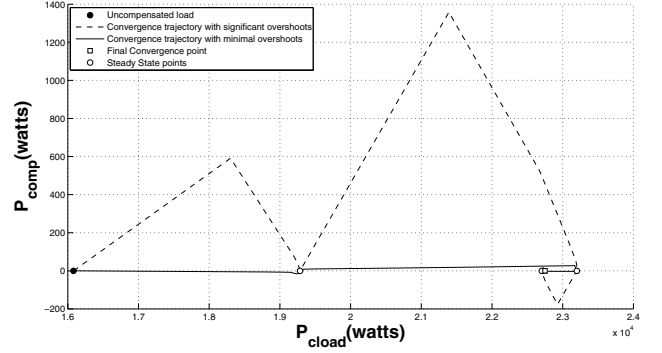


Fig. 7. Comparison of the trajectory with significant overshoots versus the trajectory with minimal overshoots.

that in steady-state $P_{comp} = 0$, so that all steady-state points lie on the quad-Fryze equivalent cross section curve corresponding to $P_{comp} = 0$. Recall we use the optimal solution (dash-dot line in Fig. 6) as a benchmark for comparison and due to the near-optimal characteristic of our quad-Fryze compensation it is observed that the steady-state points (white circle markers in Fig. 6) lie very nearly on the optimum cross section curve.

D. Transient Behavior

During the adaptation process for $\alpha(k)$, the value of P_{comp} can be quite different from its desired (steady-state) value. In fact, all three power quantities — P_{line} , P_{comp} , P_{cload} — undergo a transient while $\alpha(k)$ is converging.

The transient in P_{comp} and P_{cload} is shown in Fig. 7 (dashed line). Notice that P_{comp} experiences dramatic overshoots. This behavior is unacceptable because every $P_{comp}(k)$ value of the trajectory is not desired to be quite different from the prescribed $P_{comp,desired}$. This inconvenience can be overcome by including additional temporary scaling for the value of $\gamma(k)$, but maintaining the recursion formula (35) as before, so that

$$\gamma(k) = [1 + \epsilon(k)][\alpha(k) + j\beta], \quad (39)$$

where $\epsilon(k) \rightarrow 0$ as $k \rightarrow \infty$.

We have found empirically that a reasonable choice of $\epsilon(k)$ is given by

$$\epsilon(k) = \begin{cases} \epsilon_0, & k = 0 \\ \epsilon_1 \eta_1^{k-1}, & k \geq 1. \end{cases} \quad (40)$$

Here we take care of the overshoot in the first step of the trajectory with ϵ_0 . The remaining overshoots during the first segment of the trajectory are taken care of with ϵ_1 and η_1 . Since $0 < \eta_1 < 1$, the contribution of $\epsilon(k)$ in the scaling effect of γ turns to be insignificant as k increases beyond certain value. Thus the technique (39) and (40) works well during the first adaptation stage (with $\beta_0 = 0$). To overcome the overshoot in subsequent β -search steps we chose instead to implement the change from β_i to β_{i+1} , as given by (36), not in a single step but as a sequence of smaller changes, each one of size $\frac{\beta_{i+1} - \beta_i}{100}$.

We found by trial and error that the values $\epsilon_0 = 0.037$, $\epsilon_1 = 0.0095$, and $\eta_1 = 0.67$ appear to work well in our example across a variety of $P_{cload,desired}$ values for $P_{comp,desired} = 0$ and they may not work well in other kind of examples.

The final effect of this operation can be appreciated in Figure 7 (solid line) where we can observe that the overshoots have been significantly reduced.

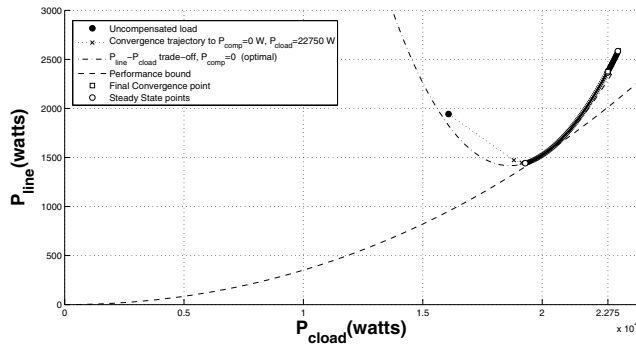


Fig. 8. Convergence trajectory with minimal overshoots of P_{comp} .

Figure 8 presents the performance of the convergence trajectory where it is evident that a smoother trajectory can be achieved with the minimization of the overshoots in comparison with that one shown in Fig. 6. In addition, observe that after the first segment of the trajectory the adaptive algorithm is very nearly on the theoretical optimum (dash-dot line).

VI. CONCLUDING REMARKS

The paper begins with a complete formulation of the problem related to the near-optimal compensation in lossy polyphase power systems where the objective in determining an adaptive near-optimal compensator based on the concept of quad-Fryze has been clearly achieved.

Near-optimal compensation is intended to get the smallest possible P_{line} for prescribed P_{comp} , P_{cload} , where in practical terms is of more interest the implementation of a compensator under lossless conditions ($P_{comp} = 0$). As a result, we obtained an adaptive compensator with the desired steady state and a manageable transient behavior, essentially independent of network information, which can track changes in load and network conditions and that is very nearly optimal at least for a linear load.

It is perhaps needed to find other methods of adjusting β maybe before full convergence of the adjustment of α . On the other hand, the need to find analytical (approximate) results that let us figure out completely the situation of why there are overshoots (mostly above $P_{comp}(\infty)$), has also to be considered in further research. In such a way, it will be required to create new strategies in minimizing these overshoots. Among them we can mention the study of what works better between using $[1 + \epsilon(k)][\alpha(k) + j\beta]$ or $[1 + \epsilon(k)]\alpha(k) + j\beta$; the necessity to find a way in selecting $\epsilon(k)$ when \mathcal{Z}_s , \mathcal{Y} are not known, i.e., select it a priori, without experimentation; or, alternatively, the idea of adjusting $\epsilon(k)$ adaptively based only on the transient P_{comp} values could be a good choice.

ACKNOWLEDGMENT

This work was supported in part by the National Science Foundation under Grants ECS-0601256 and ECS-0746310.

REFERENCES

- [1] S. Fryze, "Wirk-, Blind-, und Scheinleistung in electrischen Stromkreisen mit nichtsinusformigem Verlauf von Strom und Spannung," *Elektrotech. Z.*, Vol. 53, No. 25, pp. 596-599, June 1932.
- [2] H. Lev-Ari, A.M. Stanković, "Hilbert Space Techniques for Modeling and Compensation of Reactive Power in Energy Processing Systems," *IEEE Trans. Circuits Syst. I, Fundam. Theory Appl.*, Vol. 50, No. 4, pp. 540-556, Apr. 2003.

- [3] H. Lev-Ari, A.M. Stanković, K. Xu, M.M. Perišić, "Hilbert Space Techniques for Evaluating Trade-offs in Reactive Power Compensation," in *Proc. of the IEEE Int. Symp. on Circuits and Systems*, Vancouver, Canada, May 2004, Vol. V, pp. 976-979.
- [4] H. Lev-Ari, A.M. Stanković, "Hilbert Space Techniques for Reactive Power Compensation with Limited Current Bandwidth," *Proc. of the IEEE Int. Symp. on Circuits and Systems*, Vancouver, Canada, May 2004, Vol. V, pp. 904-907.
- [5] H. Lev-Ari, A.M. Stanković, "Optimizing Power Flows in Lossy Polyphase Systems: Effects of Source Impedance," *7th International Workshop on Power Definitions and Measurements under Non-Sinusoidal Conditions*, Cagliari, Italy, July 2006, pp. 78-83.
- [6] H. Lev-Ari, A.M. Stanković, "Fundamental Performance Limits in Lossy Polyphase Systems: Apparent Power and Optimal Compensation," *IEEE Int. Symp. on Circuits and Systems*, May 2007, Vol. 27, No. 30, pp. 61-64.